NANO LETTERS

Letter

pubs.acs.org/NanoLett

Single-Crystal Poly(3,4-ethylenedioxythiophene) Nanowires with Ultrahigh Conductivity

Boram Cho,[†] Kyung S. Park,[†] Jangmi Baek, Hyun S. Oh, Yong-Eun Koo Lee, and Myung M. Sung*

Department of Chemistry, Hanyang University, Seoul 133-791, Korea

Supporting Information

ABSTRACT: We developed single-crystal poly(3,4-ethylenedioxythiopene) (PEDOT) nanowires with ultrahigh conductivity using liquid-bridge-mediated nanotransfer printing with vapor phase polymerization. The single-crystal PEDOT nanowires are formed from 3,4-ethylenedioxythiophene (EDOT) monomers that are self-assembled and crystallized during vapor phase polymerization process within nanoscale channels of a mold having $FeCl_3$ catalysts. These PEDOT nanowires, aligned according to the pattern in the mold, are then directly transferred to specific positions on a substrate to generate a nanowire array by a direct printing process. The PEDOT nanowires have closely packed single-crystalline structures with orthorhombic lattice units. The conductivity of the single-crystal PEDOT nanowires is an average of 7619 S/cm with the highest up to 8797 S/cm which remarkably exceeds literature values of PEDOT nanostructures/thin films. Such distinct conductivity enhancement of single-crystal PEDOT nanowires can be attributed to improved carrier mobility in PEDOT nanowires. To demonstrate usefulness of single-crystal PEDOT nanowires, we fabricated an organic nanowire field-effect transistor array contacting the ultrahigh conductive PEDOT nanowires as metal electrodes.

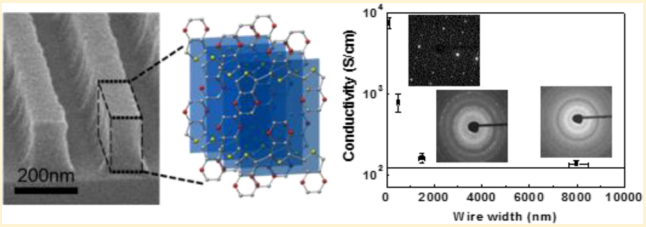

KEYWORDS: *PEDOT, conducting polymer, single-crystal organic nanowires, direct printing, vapor phase polymerization*

Conjugated organic polymers with heterocyclic structures have good electrical conductivity, excellent transmittance in the visible frequency, structural flexibility, and tunable electronic properties.[1,2] The conducting polymers have shown great promise in flexible, inexpensive, large-area applications such as flexible displays, radio frequency identification devices (RFIDs), photovoltaic arrays, smart cards, nonvolatile memory, and sensors.[3−6] Among the heterocyclic conducting polymers, poly(3,4-ethylenedioxythiophene) (PEDOT) is a unique material that has received significant attention for its potential applications as transparent and flexible electrodes in organic transistors, photovoltaic devices, optical displays, organic light emitting diodes, and biosensors owing to its high conductivity, good transparency, excellent thermal and atmospheric stability, and low redox potential.[7−11]

Since PEDOT was first synthesized at the Bayer research laboratory, many derivatives have been developed by oxidative chemical and electrochemical polymerization methods using various kinds of monomers, oxidants, and counterions.[12−14] The electrical conductivity of PEDOT and its derivatives has increased from an initial value of 2 S cm^{-1} up to the value exceeding 4500 S cm^{-1}.[14,15] Such variation of the conductivity by several orders of magnitude is largely caused by the nature of various dopant anions, e.g., Cl^-, PF_6^-, tosylate, poly(styrenesulfonate), sulfated poly(β-hydroxyether), etc.[14] These polymers with enhanced electrical conductivities have demonstrated many traditional signatures of metallic conductivity.[16−19] The conductivity of the PEDOT also strongly depends on the degree of crystallinity, confirming the general trend that the interchain charge carrier mobility in a given conducting polymer is significantly affected by chain alignment and crystalline state of the polymer.[15,20,21] This suggests that another method of achieving a higher level of conductivity in the PEDOT is to increase crystallinity. Single-crystal PEDOT would be particularly useful because it would show intrinsic charge-transport properties and the highest performance due to the perfect order of polymer chains, the absence of grain boundaries, the good interface of contact, and the minimal concentration of charge traps. However, the crystalline order of PEDOT and its derivatives has been limited—usually amorphous or paracrystalline, which leads to scattering, trapping at defects, and localization of charge carriers.[15,20,22]

Herein, we developed single-crystal PEDOT nanowire arrays using nanotransfer direct printing of the PEDOT nanowires produced by vapor phase polymerization (VPP) of 3,4-ethylenedioxythiophene (EDOT) in the presence of catalyst, $FeCl_3$. Importantly, we achieved simultaneously the synthesis, alignment, and patterning of single-crystal PEDOT nanowires. The PEDOT nanowires—produced inside one-dimensional nanoconfinements, i.e., nanoscale channels of a mold, exhibit high crystalline nature and ultrahigh conductivity (≈8000 S cm^{-1}). Furthermore, the single-crystal PEDOT nanowires can

Received: February 27, 2014
Revised: April 26, 2014
Published: May 21, 2014

   dx.doi.org/10.1021/nl500748y | *Nano Lett.* 2014, 14, 3321−3327

be properly integrated into organic nanowire devices in such a way that a group of nanowires, aligned with a preset interspace according to the pattern in the mold, is directly transferred on the device substrate.

Figure 1a illustrates the procedure used to generate a single-crystal PEDOT nanowire arrays by liquid-bridge-mediated nanotransfer molding (LB-nTM) process in combination with VPP of EDOT.[23] A mold is fabricated by casting polyurethane acrylate (PUA) on a silicon wafer with a nanoscale line pattern of resists (Figure 1b). Ferric chloride ($FeCl_3$) solution fills only the channels of the PUA mold due to selective inking based on discontinuous dewetting.[24] The thickness of the $FeCl_3$ solution in each of the nanoscale channels is about 10 nm after drying at mild temperature (50 °C) for <10 min (Figure 1c). The dried mold having $FeCl_3$ is then exposed to EDOT and methanol vapors concurrently in a VPP chamber at 50 °C for 20 min. The methanol vapor was exposed to make the $FeCl_3$ oxidants liquid-like states for the bottom-up growth of PEDOT.[25] The exposing time at the polymerization conditions is sufficient for terminating the PEDOT growth, indicating that the PEDOT thicknesses are mainly determined by the amount of $FeCl_3$ in the molds. The EDOT molecules are polymerized, self-assembled, and crystallized on $FeCl_3$ molecules within the nanoscale channels to form single-crystal PEDOT nanowires (Figure 1d). The single-crystal PEDOT nanowires in the mold are directly transferred on selected locations of desired substrates (Figure 1f) using liquid-bridge-mediated transfer process, as shown in Figure 1e. Subsequent washing with methanol removes the remaining $FeCl_3$ molecules resulting in an array of high-quality single-crystal PEDOT nanowires (Figure 1g).

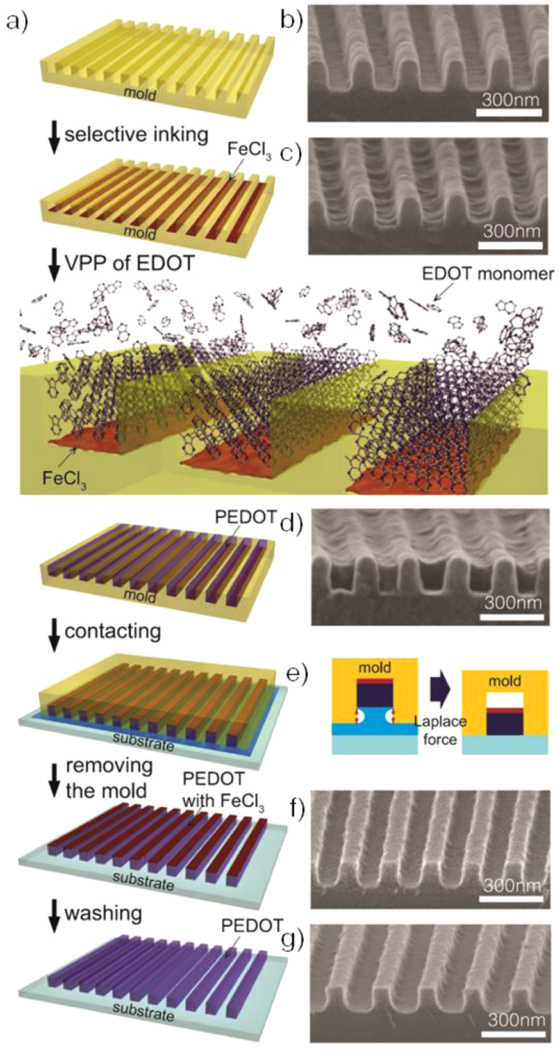

Figure 1. Fabrication of a single-crystal PEDOT nanowire array. (a) Schematic illustration of the procedure used to fabricate a single-crystal PEDOT nanowire array on a substrate using LB-nTM with VPP. (b) An SEM image of a PUA mold with a nanoscale pattern. (c) An SEM image of the mold filled with $FeCl_3$ catalyst molecules. (d) An SEM image of the mold filled with single-crystal PEDOT nanowires grown via VPP process. (e) Schematic illustration of a liquid bridge formed by a polar liquid layer between PEDOT nanowires and a substrate. (f) An SEM image of a single-crystal PEDOT nanowire array on a Si substrate before washing. (g) An SEM image of a single-crystal PEDOT nanowire array on a Si substrate after washing with methanol to remove residual $FeCl_3$.

An SEM image of a single-crystal PEDOT nanowire array—fabricated using a mold having a line pattern with a period of 200 nm (100 nm-wide parallel lines, 150 nm-deep, and 100 nm-wide spaces between the lines)—clearly shows that the nanowires, each with a width of 95 nm and a height of 100 nm, are perfectly aligned to form a 200 nm period array on the substrate (Figure 2a). Note that each nanoscale channel of the

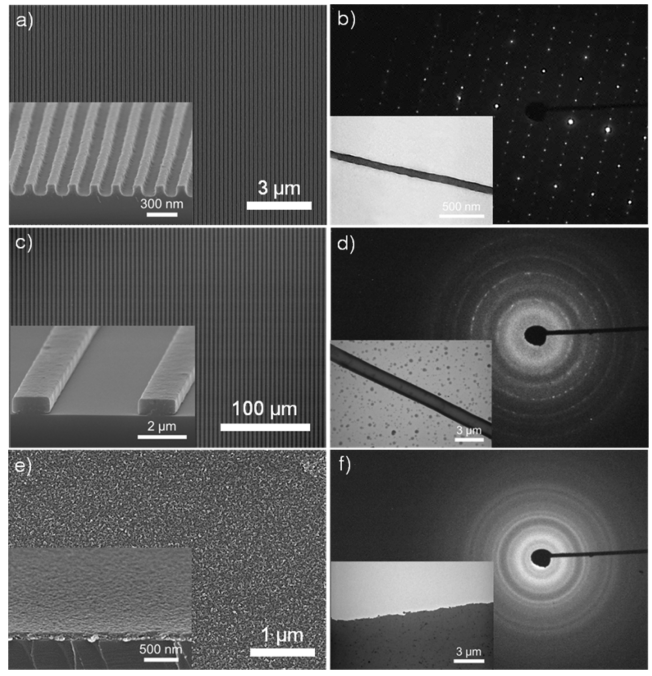

Figure 2. Electron microscopic images and SAED patterns of PEDOT nanowires, microribbons, and thin film. (a) An SEM image of a PEDOT nanowire array (white) fabricated by LB-nTM on a Si substrate (black). Inset: corresponding perspective magnified view of the nanowire array. (b) An SAED pattern and the corresponding TEM image (inset) of the PEDOT nanowire. The diffraction pattern shows the single-crystalline nature. (c) An SEM image of a PEDOT microribbon array. Inset: corresponding perspective magnified view of the microribbon array. (d) An SAED pattern and the corresponding TEM image (inset) of a PEDOT microribbon, which indicates the semicrystalline nature. (e) An SEM image of a PEDOT thin film. Inset: corresponding perspective magnified view of the thin film. (f) An SAED pattern and the corresponding TEM image of the PEDOT thin film, which indicates amorphous nature.

dx.doi.org/10.1021/nl500748y | Nano Lett. 2014, 14, 3321−3327

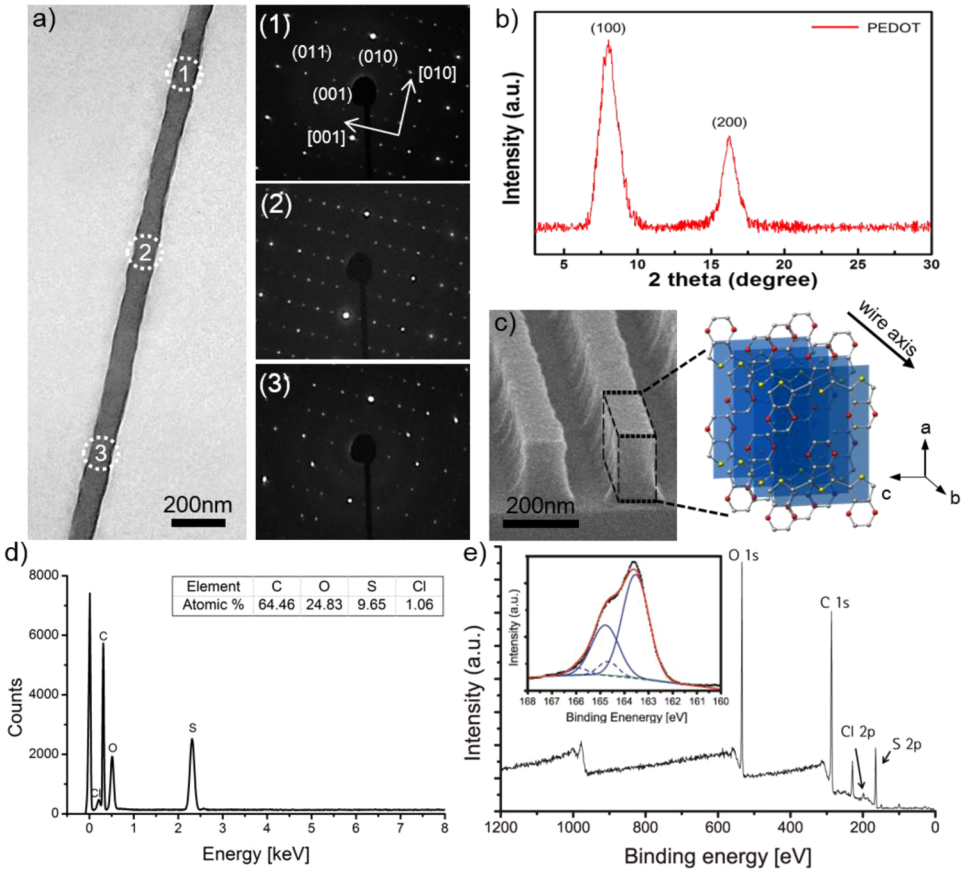

Figure 3. Characterization of single-crystal PEDOT nanowires. (a) A TEM image of a PEDOT nanowire and the corresponding SAED patterns corresponding to three different areas of the PEDOT nanowire. Each area shows the single-crystalline nature. (b) An XRD pattern of a PEDOT nanowire array fabricated on a Si substrates by LB-nTM. (c) Schematic representation of the crystal structure of the single-crystal PEDOT nanowire along the nanowire direction. (d) An EDX spectrum of a PEDOT nanowire array. (e) An XPS spectrum of the PEDOT nanowire array. The inset shows a high-resolution spectrum of the S(2p) signal of the PEDOT nanowires.

mold is filled with a 10 nm-thick $FeCl_3$ oxidant layer. The height of the PEDOT nanowire is mainly determined by the amount of $FeCl_3$ oxidants in the molds because the polymerization time is sufficient for terminating the PEDOT growth. The crystalline structures of the PEDOT nanowires were examined by selective-area electron diffraction (SAED). A SAED pattern and a corresponding TEM image (inset) of the PEDOT nanowire are shown in Figure 2b. The SAED pattern presents very well-ordered, bright Bragg diffraction spots, indicating that the PEDOT nanowire is of single-crystalline nature.

For comparison, PEDOT microribbons and PEDOT thin films were also fabricated by the same method, using a micropatterned mold with 4 μm-wide parallel lines and 2 μm-wide spaces between the lines and using a nonpatterned mold, respectively. SEM images of the resultant PEDOT microribbons with a width of 1.8 μm and a height of 600 nm and the thin film with a thickness of 180 nm are shown in Figure 2c,e, respectively. Note that the thicknesses of the $FeCl_3$ oxidants in the micro- and nonpatterned molds are 60 and 20 nm, respectively. SAED patterns and TEM images of the microribbon and the thin film are shown in Figure 2d,f, respectively. The SAED pattern of the PEDOT microribbon shows discrete diffraction spots in each Debye ring, indicating that they have a preferred-oriented polycrystalline ordering. Ring-type diffraction was observed for the PEDOT thin film, which indicates that it is amorphous and random-oriented polycrystalline. These results could be attributed to formation of the PEDOT in environments with different spacial restrictions during the VPP process. It can therefore be concluded that nanoconfinement effect provided by the nanochannels in the mold is crucial for the formation of the single-crystal PEDOT nanowires.

The single crystalline nature of the PEDOT nanowires was confirmed by the SAED analysis (Figure 3a), which was performed at three different positions along a PEDOT nanowire. The SAED patterns were obtained perpendicular to the length axis of the PEDOT nanowire, presenting very well-ordered diffraction spots. A repetition unit of 7.91 Å along the polymer chain direction and a repetition unit of 4.64 Å along the $\pi-\pi$ stacking direction were observed. These data indicate that the PEDOT nanowire has an orthorhombic crystal unit cell with lattice constants of a = 11.01 Å, b = 4.64 Å, and c = 7.91 Å and that it forms along the [010] direction on the substrate, coinciding with the (100) projection from XRD results (Figure 3b). Thus, we can draw a schematic representation of the crystal structure of the single-crystal PEDOT nanowire along the nanowire direction, as shown in Figure 3c. The lateral chain spacing (a) and $\pi-\pi$ stacking distance (b) are smaller than those of the previously reported PEDOT with different dopants and crystallinity, probably due to the relatively small (Cl^-) dopant and the favorable packing of the incoming monomers within the nanoscale channels.[22,26]

Energy dispersive X-ray spectroscopy (EDX) analysis was performed to determine the composition of the PEDOT

dx.doi.org/10.1021/nl500748y | Nano Lett. 2014, 14, 3321−3327

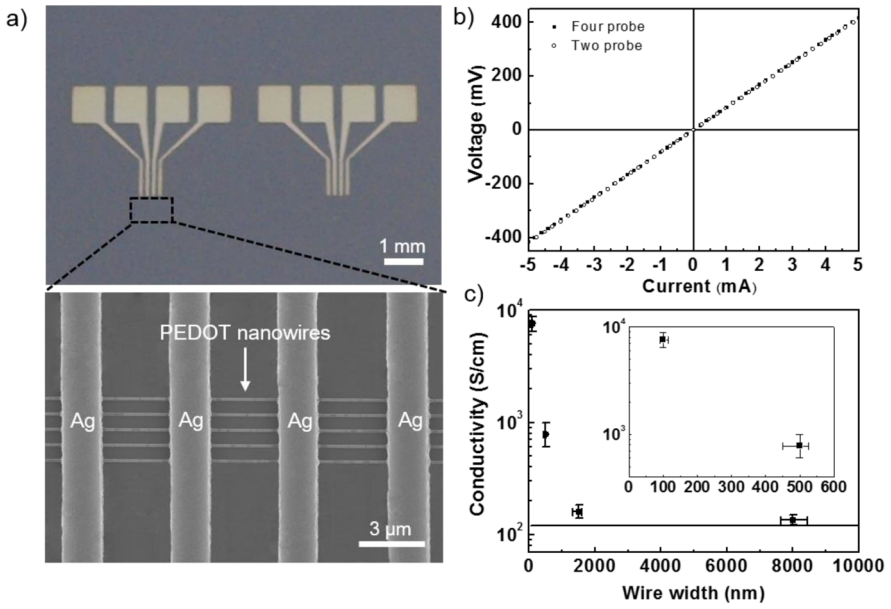

Figure 4. Conductivity measurements of PEDOT nanowires, microribbons, and thin films. (a) An optical microscopy image of a device for four point resistivity measurements (top). An SEM image of the dotted rectangle in the optical microscopy image: a magnified view showing a 5 PEDOT nanowire array connected by four Ag electrodes (bottom). (b) *V*–*I* plots for an array of 5 PEDOT nanowires. (c) Conductivity of the PEDOT nanowires or microribbons as a function of the width. The solid line indicates the conductivity of the PEDOT thin films.

nanowires fabricated by this process. An EDX spectrum obtained from the 95 nm-wide and 100 nm-thick single-crystal PEDOT nanowires displays the characteristic peaks for carbon, oxygen, sulfur, and chlorine but none for iron, as shown in Figure 3d. Note that iron peaks are supposed to appear at 6.4 and 7.1 eV. The atomic concentrations for C, O, S, and Cl are 64.46%, 24.83%, 9.65%, and 1.06%, respectively. These results give the C/O/S ratio of 6:2:1 that matches with the atomic ratio of pristine PEDOT. It should be noted that there was no external doping of Cl, and therefore the Cl should originate from $FeCl_3$. It looks like that the Fe was efficiently removed by methanol washing but the Cl counteranions remained in the PEDOT crystals so as to serve as a major dopant. There is one chloride for 10 thiophene rings on average, and the estimated doping level is 10%. This conclusion is further confirmed by X-ray photoelectron spectroscopy (XPS) analysis, as shown in Figure 3e. The estimated elemental composition of the PEDOT nanowires by the XPS analysis is C 65.09%, O 22.61%, S 11.12%, and Cl 1.18%. As a result, the atomic ratio of S to Cl is approximately 10:1, which is consistent with the estimated doping level by EDX. Moreover the thiophene S(2p) signal in the high-resolution XPS spectrum also allows us to evaluate the doping level, utilizing the amount of positive charges—induced by anion (Cl^-) dopants—on the thiophene rings.[27−29] The high-resolution spectrum (Figure 3e, inset) shows the natural S(2p) region consisting of a spin-split doublet, $S(p_{1/2,3/2})$, with the energy splitting of 1.2 eV (blue solid lines).[30] The peaks include two S(2p) doublets with the blue solid and dotted lines denoting neutral and partially oxidized S atoms, respectively.[30] It is likely that these doublets correspond to undoped (163.4 eV for $S(2p_{3/2})$, 164.6 eV for $S(2p_{1/2})$) and doped (164.7 eV for $S(2p_{3/2})$, 165.9 eV for $S(2p_{1/2})$) sulfur atoms. These results revealed the doping level of about 10%—estimated from the area ratio of doped/undoped peaks—for the PEDOT nanowires, which is consistent with the EDX and XPS data. For comparison, the PEDOT thin films and microribbons were also analyzed by EDX and XPS, which results in the same doping levels (≈10%) as that of the nanowires. (Figure S1)

The conductivity of the single-crystal PEDOT nanowires was measured using a four-point resistivity measurement technique. An array of the five PEDOT nanowires—each having 95 nm width, 100 nm height, and 100 μm length—was fabricated on a 200 nm-thick SiO_2 substrate using LB-nTM with VPP. Next, a metal electrode array made of four 1.5 μm-thick Ag microribbons was perpendicularly defined to contact the PEDOT nanowires on the substrate by LB-nTM using a micropatterned mold with 3 μm-wide parallel lines and 2 μm-wide spaces (Figure 4a, bottom). Finally, 200 nm-thick Au pads were deposited by evaporation using a shadow mask for electrical measurements (Figure 4a, top). More than 20 PEDOT nanowire devices were fabricated for measuring the resistivities of the nanowires. Figure 4b shows the linear voltage (V) versus current (I) curve for the highest conductive PEDOT nanowire device. More than 20 PEDOT nanowire devices were fabricated and voltage (V) versus current (I) plots were obtained using a four point probe to measure the resistance of the devices. The resistivity and conductivity of the PEDOT nanowires in each device were then calculated using the measured resistance value of the device and the dimension of the five PEDOT nanowires (each having 95 nm width, 100 nm height, and 3.5 μm length). Figure 4b shows a linear V versus I plot obtained for the highest conductive PEDOT nanowire device which showed the resistivity value of 1.13×10^{-4} Ωcm, equivalent to the conductivity value of 8797 S cm^{-1}. We also measured the resistivity from the two-point measurement using the inner pair of electrodes is about 1.19×10^{-4} Ωcm which is almost identical to that obtained from the four-point probe, indicating that the contact resistance at the interface between the nanowires and the Ag metal pads is negligible. The conductivity measurements of the 20 PEDOT nanowire devices result in an average value of 7619 S cm^{-1} with the standard deviation of 771.6 S cm^{-1}. Significantly, the conductivity of the single-crystal PEDOT nanowires is higher than typical PEDOT

dx.doi.org/10.1021/nl500748y | *Nano Lett.* 2014, 14, 3321−3327

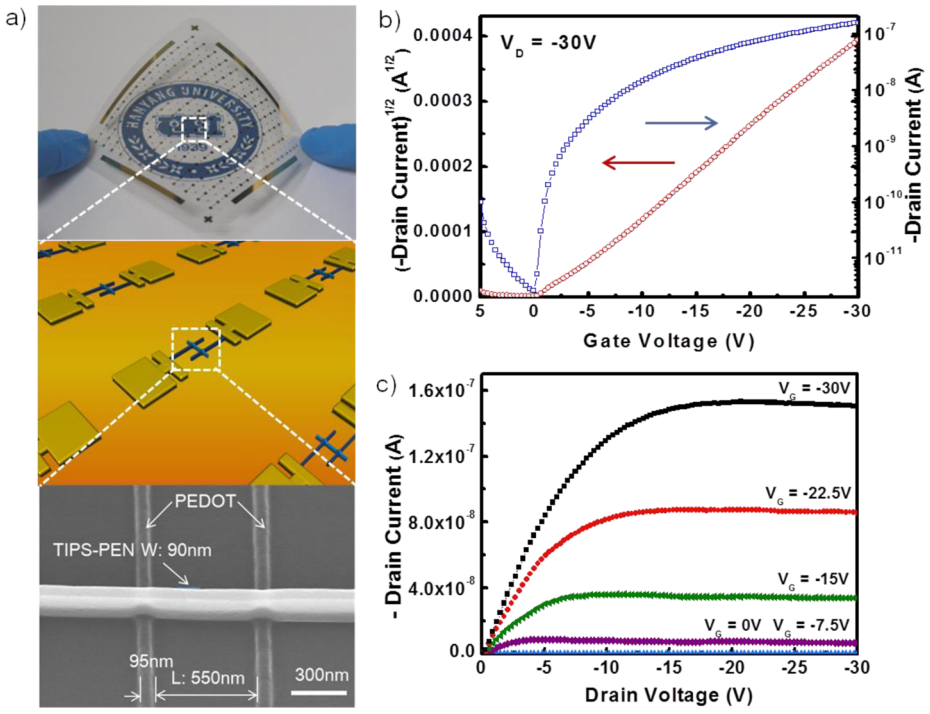

Figure 5. Fabrication and characterization of organic nanowire FETs. (a) A photograph of an array of FETs on a flexible substrate: Each FET uses a single-crystal TIPS-PEN nanowire as p-type active channel and a pair of single-crystal PEDOT nanowires as source and drain electrodes (top). A schematic of the FET array (middle). An SEM image of a single TIPS-PEN nanowire with a pair of PEDOT nanowires in the FET array: A 30° tilted, magnified view of the white dotted rectangle in the schematic (bottom). (b) Drain current−gate voltage (I_D−V_G) transfer curves (V_D = −30 V) of TIPS-PEN nanowire FETs. (c) Drain current−drain voltage (I_D−V_D) output curves obtained from the same device.

thin films by almost 2 orders of magnitude and is the highest among the values achieved in PEDOT and its derivatives.[15,31,32] For comparison, the PEDOT submicroribbons and microribbons were fabricated by LB-nTM for conductivity measurements using the same method as that used for the nanowires. Note all PEDOT samples for conductivity measurement have the same thickness of about 100 nm. Figure 4c displays the variation in the conductivity of the PEDOT nanowires or microribbons with respect to their width. The conductivity rapidly decreases with increasing width and levels off to the conductivity value of PEDOT thin films at 8000 nm. Unambiguously, our study shows a very strong increase in the conductivity for the single-crystal PEDOT nanowires. A material's conductivity (σ) is generally known to be proportional to the product of the carrier density (N) and the carrier mobility (μ) and can be expressed as $\sigma = qN\mu$, where q is the elementary charge. From this relationship, it is possible to expect that the outstanding conductivity of the single-crystal PEDOT nanowires can be generated from the enhanced doping level and/or crystallinity. As the estimated doping level of the single-crystal PEDOT nanowires is the same as that of the PEDOT thin films or microribbons, about 10% by the EDX and XPS results, the carrier mobility (or crystallinity) seems to play a major role for the enhanced conductivity of the single-crystal nanowires. The carrier mobility (μ) of the single-crystal PEDOT nanowires can be estimated by using the equation $\mu = \sigma/qN$. The carrier density (N) of the VPP-grown PEDOT structures is calculated to be approximately 6.23×10^{20} cm^{-3} by using the relation, $N = dN_An/FW$, where d = 1.45 g/cm^3, FW = 140 g/mol, and N_A is Avogadro's number.[29,31,32] Using this N value, the carrier mobility of the nanowires showing the highest conductivity (8797 S cm^{-1}) becomes 88.08 cm^2 V^{-1} s^{-1}. Notably, this carrier mobility value is the highest among reported values for PEDOT and its derivatives.[31,33] Such high enhancement in the mobility of the single-crystal PEDOT nanowires strongly suggests that their high crystalline structure with a small π−π stacking distance mainly contributes to the ultrahigh conductivity.

In order to demonstrate usefulness of ultrahigh conductive PEDOT nanowires, a large-scale array of field-effect transistors (FETs) was fabricated on 5 × 5 cm^2 poly(ether sulfone) (PES) substrates using single-crystal 6,13-bis(triisopropylsilylethynyl)-pentacene (TIPS-PEN) nanowires as p-type active channels and single-crystal PEDOT nanowires as source and drain electrodes for bottom gate and bottom contact configuration (Figure 5a, top). A 150 nm-thick indium−tin oxide (ITO) gate electrode and a 200 nm-thick SiO_2 dielectric layer were formed on a PES substrate by sputter deposition. A pair of the 95 nm-wide PEDOT nanowires with 550 nm-wide space between them was then deployed on the substrate by using LB-nTM with VPP. Next, an array of the 90 nm-wide and 135 nm-high TIPS-PEN nanowires as p-type active channel layers was defined on the substrate by LB-nTM contacting the PEDOT nanowire electrodes.[34] Finally, the PEDOT nanowire source and drain electrodes were electrically connected by evaporation of 200 nm-thick Au using a shadow mask. A schematic illustration of the array is shown in Figure 5a (middle). Figure 5a (bottom) shows an SEM image of a part of single FET—the single-crystal TIPS-PEN nanowire in contact with two single-crystal PEDOT nanowires functioning as source and drain electrodes. Figure 5b,c presents typical drain current−gate voltage (I_D−V_G) transfer curves and drain current−drain voltage (I_D−V_D) output curves measured in air, respectively, for the FETs with single TIPS-PEN nanowire in the channel

dx.doi.org/10.1021/nl500748y | Nano Lett. 2014, 14, 3321−3327

region. The FETs were well-modulated, as typical p-type transistors, in accordance with the gate voltage and exhibited clear saturation behavior. The field-effect mobility (μ) and threshold voltage (V_{th}) were calculated in the saturation regime (V_D = −30 V) by plotting the square root of the drain current versus the gate voltage using $I_D = (WC_i/2L)\mu(V_G - V_{th})^2$, where C_i is the capacitance/unit area of the gate dielectric layer (15 nF/cm^2), and W and L are the channel width and length, respectively.

The TIPS-PEN FETs with single-crystal PEDOT nanowires as source/drain contacts showed excellent device performance, with a field-effect mobility of 0.15 cm^2 V^{-1} s^{-1}, an on/off current ratio of ∼10^4, and a threshold voltage of −2.5 V. We note that these FETs have a field-effect mobility that is lower than those of the FETs with micrometer-size metal electrodes due to a smaller contact area between the active nanowires and the nanowire electrodes.[34] However, this FET performance is comparable to that of the FETs containing Ag nanowire electrodes (Figure S2). Due to its high-metallic properties, the single-crystal PEDOT nanowires, fabricated using LB-nTM with VPP, are very applicable as metal components for transparent and flexible electronics.

In summary, we have developed single-crystal PEDOT nanowires with ultrahigh conductivity by using a direct printing method combined with vapor phase polymerization process. In this method, EDOT monomers are oxidized, self-assembled, and crystallized in nanoscale channels of the mold containing the $FeCl_3$ catalysts, producing an array of single-crystal PEDOT nanowires. Thus, formed PEDOT nanowires are of single crystal nature, with closer lateral chain spacing and $\pi-\pi$ stacking distance than those of most PEDOT systems. The single-crystal PEDOT nanowires have ultrahigh conductivity up to 8797 S cm^{-1} in comparison to the microribbons and thin films that were prepared by the same method except the dimension of patterned channels. This increase in conductivity of the single-crystal PEDOT nanowires is due to their high-crystalline structures resulting in carrier mobility enhancement. It is suggested that the nanoscale channels of a mold strongly affect to form single-crystal PEDOT nanowires of such ultrahigh conductivity by this method. Moreover, single-crystal PEDOT nanowires were successfully demonstrated for their use as flexible metal electrodes in high-integrated organic field-effect transistors. The single-crystal PEDOT nanowires, due to their ultrahigh conductivity and their ability to be printed on the substrates, could potentially be used in all organic nanowire electronics for transparent, flexible, inexpensive, and large-area applications.

■ ASSOCIATED CONTENT

Supporting Information

Figures S1 and S2 and materials and detailed experimental methods. This material is available free of charge via the Internet at http://pubs.acs.org.

■ AUTHOR INFORMATION

Corresponding Author

*E-mail: smm@hanyang.ac.kr.

Author Contributions

†These authors contributed equally.

Notes

The authors declare no competing financial interest.

■ ACKNOWLEDGMENTS

This work was supported by the National Research Foundation (NRF) grant funded by the Korea government (MEST) (no. 2009-0092807), and the Global Frontier R&D Program on the Center for Multiscale Energy System (no. 2011-0031562) and Nano· Material Technology Development Program (2012M3A7B4034985) through the National Research Foundation of Korea (NRF) funded by the Ministry of Science, ICT & Future Planning, Korea. We thank the Korea Basic Science Institute (KBSI) for allowing us to use their EF-TEM.

■ REFERENCES

(1) Dennler, G.; Sariciftci, N. S. *Proc. IEEE* **2005**, *93*, 1429−1439.
(2) Facchetti, A. *Chem. Mater.* **2011**, *23*, 733−758.
(3) Heeger, A. J. *Angew. Chem., Int. Ed.* **2001**, *40*, 2591−2611.
(4) Wallace, G. G.; Campbell, T. E.; Innis, P. C. *Fiber Polym.* **2007**, *8*, 135−142.
(5) Ling, Q. D.; Liaw, D. J.; Zhu, C. X.; Chan, D. S. H.; Kang, E. T.; Neoh, K. G. *Prog. Polym. Sci.* **2008**, *33*, 917−978.
(6) Cheng, Y. J.; Yang, S. H.; Hsu, C. S. *Chem. Rev.* **2009**, *109*, 5868−5923.
(7) Sirringhaus, H.; Kawase, T.; Friend, R. H.; Shimoda, T.; Inbasekaran, M.; Wu, W.; Woo, E. P. *Science* **2000**, *290*, 2123−2126.
(8) Aernouts, T.; Vanlaeke, P.; Geens, W.; Poortmans, J.; Heremans, P.; Borghs, S.; Mertens, R.; Andriessen, R.; Leenders, L. *Thin Solid Films* **2004**, *451*, 22−25.
(9) Admassie, S.; Zhang, F. L.; Manoj, A. G.; Svensson, M.; Andersson, M. R.; Inganas, O. *Sol. Energy Mater. Sol. Cells* **2006**, *90*, 133−141.
(10) Lloyd, M. T.; Mayer, A. C.; Tayi, A. S.; Bowen, A. M.; Kasen, T. G.; Herman, D. J.; Mourey, D. A.; Anthony, J. E.; Malliaras, G. G. *Org. Electro.* **2006**, *7*, 243−248.
(11) Yoon, H.; Chang, M.; Jang, J. *Adv. Funct. Mater.* **2007**, *17*, 431−436.
(12) Jonas, F.; Heywang, G.; Schmidtberg W. (Bayer AG). Novel polythiophenes, process for their preparation, and their use. DE 3813589 A1, April 22, 1988.
(13) Heywang, G.; Jonas, F.; Heinze J.; Dietrich M. (Bayer AG), New polythiophene, process for their production and their use. DE 3843412 A1, December 23, 1988.
(14) Groenendaal, B. L.; Jonas, F.; Freitag, D.; Pielartzik, H.; Reynolds, J. R. *Adv. Mater.* **2000**, *12*, 481−494.
(15) Kim, J. Y.; Kwon, M. H.; Min, Y. K.; Kwon, S.; Ihm, D. W. *Adv. Mater.* **2007**, *19*, 3501−3506.
(16) Kim, T. Y.; Park, C. M.; Kim, J. E.; Suh, K. S. *Synth. Met.* **2005**, *149*, 169−174.
(17) Feng, W.; Li, Y.; Wu, J.; Noda, H.; Fujii, A.; Ozaki, M.; Yoshino, K. *J. Phys.; Condens. Matter* **2007**, *19*, 186220.
(18) Le Truong, T.; Kim, D. O.; Lee, Y.; Lee, T. W.; Park, J. J.; Pu, L.; Nam, J. D. *Thin Solid Films* **2008**, *516*, 6020−6027.
(19) Ali, M. A.; Kim, H. H.; Lee, C. Y.; Soh, H. S.; Lee, J. G. *Met. Mater. Int.* **2009**, *15*, 977−981.
(20) Su, K.; Nuraje, N.; Zhang, L. Z.; Chu, I. W.; Peetz, R. M.; Matsui, H.; Yang, N. L. *Adv. Mater.* **2007**, *19*, 669−672.
(21) Zuber, K.; Fabretto, M.; Hall, C.; Murphy, P. *Macromol. Rapid Commun.* **2008**, *29*, 1503−1508.
(22) Niu, L.; Kvarnstrom, C.; Froberg, K.; Ivaska, A. *Synth. Met.* **2001**, *122*, 425−429.
(23) Hwang, J. K.; Cho, S.; Dang, J. M.; Kwak, E. B.; Song, K.; Moon, J.; Sung, M. M. *Nat. Nanotechnol.* **2010**, *5*, 742−748.
(24) Jackman, R. J.; Duffy, D. C.; Ostuni, E.; Willmore, N. D.; Whitesides, G. M. *Anal. Chem.* **1998**, *70*, 2280−2287.
(25) Evans, D.; Fabretto, M.; Mueller, M.; Zuber, K.; Short, R.; Murphy, P. *J. Mater. Chem.* **2012**, *22*, 14889.
(26) Aasmundtveit, K. E.; Samuelsen, E. J.; Inganas, O.; Pettersson, L. A. A.; Johansson, T.; Ferrer, S. *Synth. Met.* **2000**, *113*, 93−97.
(27) Yoon, H.; Hong, J. Y.; Jang, J. *Small* **2007**, *3*, 1774−1783.

(28) Bubnova, O.; Khan, Z. U.; Malti, A.; Braun, S.; Fahlman, M.; Berggren, M.; Crispin, X. *Nat. Mater.* **2011**, *10*, 429−433.
(29) Shirai, Y.; Takami, S.; Lasmono, S.; Iwai, H.; Chikyow, T.; Wakayama, Y. *J. Polym. Sci., Part B: Polym. Phys.* **2011**, *49*, 1762−1768.
(30) Sakmeche, N.; Aeiyach, S.; Aaron, J. J.; Jouini, M.; Lacroix, J. C.; Lacaze, P. C. *Langmuir* **1999**, *15*, 2566−2574.
(31) Winther-Jensen, B.; Forsyth, M.; West, K.; Andreasen, J. W.; Wallace, G.; MacFarlane, D. R. *Org. Electron.* **2007**, *8*, 796−800.
(32) Elschner, A.; Kirchmeyer, S.; Lövenich, W.; Merker, U.; Reuter, K. *PEDOT: Principles and Applications of an Intrinsically Conductive Polymer*; CRC Press: Boca Raton, FL, 2011; p 147.
(33) Ashizawa, S.; Shinohara, Y.; Shindo, H.; Watanabe, Y.; Okuzaki, H. *Synth. Met.* **2005**, *153*, 41−44.
(34) Park, K. S.; Cho, B.; Baek, J.; Hwang, J. K.; Lee, H.; Sung, M. M. *Adv. Funct. Mater.* **2013**, *23*, 4776−4784.
(35) Ishizaka, A.; Shiraki, Y. *J. Electrochem. Soc.* **1986**, *133*, 666−671.